Heterogeneous crystallization of dicalcium phosphate dihydrate on titanium surfaces

C. COMBES, M. FRÈCHE, C. REY
INPT-ENSCT, Laboratoire des Matériaux, Equipe Physico-Chimie des Solides, UPRESA CNRS 5071, 38 rue des 36 Ponts, 31400 Toulouse, France

B. BISCANS
INPT-ENSIGC, Laboratoire de Génie Chimique, UMR CNRS 5503, 18 Chemin de la Loge, 31078 Toulouse Cédex, France

The kinetics of nucleation and crystal growth of dicalcium phosphate dihydrate (DCPD, $CaHPO_4$. $2H_2O$) on titanium powders with different grain sizes have been investigated using the constant composition crystal growth method at 37 °C and pH = 5.50. Nucleation is independent of titanium powder size while crystal growth rate is strongly size-dependent. A minimum relative supersaturation ratio, σ_{min}, required in the system for a detectable crystal growth rate to occur, taking into account the presence of the foreign substrate in the system, was determined. Based on the kinetic data and on the various characterizations by X-ray photoelectron spectroscopy and by scanning electron microscopy, we propose a crystal growth kinetic equation as a function of two parameters: the size of the substrate and the excess of supersaturation ($\sigma - \sigma_{min}$) which is squared, indicating a spiral growth mechanism.

1. Introduction

The precipitation of calcium phosphate salts from aqueous solutions is involved in biological calcification, in the environment and in many industrial processes. The study of the kinetics of calcium phosphate crystallization from supersaturated solutions is of great interest to further understanding of the process of mineralization that might take place, after the implantation of a prosthesis, to improve its attachment and its long-term residence in hard tissues (bone and teeth). Among the various biomaterials available, titanium metal is widely used in hip protheses and dental implants [1] because of its mechanical properties and corrosion resistance related to its protecting superficial oxide film [2]. The surgical trauma associated with the implantation of a prosthesis *in vivo* induces locally acidic pHs [3] that may favor the initial formation of dicalcium phosphate dihydrate ($CaHPO_4$. $2H_2O$), hereafter called DCPD or brushite, one of the most stable calcium phosphate salts in acidic solutions. Indeed, DCPD has been proposed as one of calcium phosphate's precursors in the formation of apatite during the mineralization of bone [4, 5]. Thus, the interaction of DCPD with titanium metal may also be an essential aspect of the integration of a titanium implant into bone tissues. In this work, we used the constant composition crystal growth method in metastable supersaturated solutions at various relative supersaturation ratios. This experimental technique consists of seeding supersaturated solutions and could be employed to elucidate the mechanisms encountered in the deposition of sparingly soluble salts on various substrate surfaces [6–8]. The constant composition method allowed rates to be studied over extended periods of time with constant driving forces, i.e. constant temperature, pH, ionic strength and concentrations. In order to determine the role of the titanium surface in the process of calcification, the heterogeneous nucleation and growth of DCPD on titanium powders of different grain sizes was studied, *in vitro*, at 37 °C and pH = 5.50. We disposed of four ranges of titanium particle size to test the influence of the substrate size on the kinetics of nucleation and growth of DCPD on titanium grains.

First, we briefly focus on the heterogeneous nucleation theory that governs the formation of the initial nuclei on a foreign substrate and on the kinetics and mechanisms of electrolyte crystal growth.

We also report the most important experimental results concerning the characterization of samples by scanning electron microscopy (SEM) complementing the kinetic data. In the present work, the various possible mechanisms accounting for our experimental results are discussed.

2. Theory

Nucleation may occur spontaneously or it may be induced artificially by any foreign surface. These two

Correspondence should be addressed to: Dr M. Frèche, INPT-ENSCT, Laboratoire des Matériaux, Equipe Physico-Chimie des Solides, 38 rue des 36 Ponts, 31400 Toulouse, France.

0957–4530

cases are frequently referred to as homogeneous nucleation and heterogeneous nucleation, respectively.

2.1. Homogeneous nucleation

Basically, the nucleation step consists of the association of solute units (atoms, molecules or ions) to form ordered embryos or nuclei of different sizes which are in thermodynamic equilibrium under two opposite processes: dispersion and agglomeration governed by the positive and negative free energies corresponding, respectively, to the embryo surface, ΔG_s, and volume, ΔG_v, creation. So, an embryo can either grow or dissolve depending on its size. The net process of homogeneous nucleation results in the decrease of free energy. The free energy of formation of a spherical cluster, ΔG, of radius r is given by

$$\Delta G = \Delta G_s + \Delta G_v \quad (1)$$

with $\Delta G_s = 4r^2\gamma$ and $\Delta G_v = -(4/3)\pi r^3 \Delta G_m$. ΔG_m is the free energy difference between the molecular chemical potential of solid and liquid phases, r the nucleus radius and γ the interfacial tension.

In a given system, there is usually a period of time (the induction time τ that elapses between the achievement of supersaturation and the appearance of stable nuclei. This induction period represents the time needed to form critical nuclei and has frequently been used as a measure of the nucleation rate which corresponds to the number of nuclei formed per time and volume units. Besides, Mullin [9] reported that many authors have made the simplifying assumption that the induction period is essentially devoted to nucleus formation and can therefore be considered inversely proportional to the rate of nucleation.

The nucleus critical size represents the minimum size of a stable nucleus. Particles larger than the critical nucleus will inevitably continue to grow leading to the following stage of the precipitation: crystal growth. The radius of the critical nucleus of arbitrary geometry, r_c, is inversely proportional to the supersaturation ratio, Ω (Ω = ionic product/solubility product), of the solution as we can see in the following equation

$$r_c = 2v_m\gamma/\Delta\mu \text{ with } \Delta\mu = kT \ln\Omega \quad (2)$$

where v_m is the volume of the growth unit, γ the interfacial tension, $\Delta\mu$ the chemical potential of the reaction, k Boltzmann's constant ($k = 1.38\,10^{-23}\,\mathrm{J\,K^{-1}}$) and T the absolute temperature. The free energy corresponding to the formation of the critical nuclei, ΔG_c, is expressed as follows [9]

$$\Delta G_c = (\beta\gamma^3 {v_m}^2)/(kT \ln \Omega)^2 \quad (3)$$

where β is the shape factor ($\beta = 16\pi/3$ for a spherical nucleus and $\beta = 32$ for a cubic-shaped nucleus).

2.2. Heterogeneous nucleation

Heterogeneous nucleation is a primary nucleation process that takes place on the surface of foreign solid matter which is in contact with the supersaturated solution. As the presence of a foreign body or surface can induce nucleation at degrees of supersaturation lower than those required for spontaneous nucleation, the overall free energy change associated with the formation of a critical nucleus under heterogeneous conditions, $\Delta G_{het.}$, must be less than the corresponding free energy change associated with homogeneous nucleation, $\Delta G_{hom.}$, according to Equation 4

$$\Delta G_{het.} = \phi \Delta G_{hom.} \quad (4)$$

where the factor ϕ is less than unity and is related to the contact angle θ between the nucleus and the foreign substrate, see Equation 5 [9]

$$\phi = (2 + \cos\theta)(1 - \cos\theta)^2/4 \quad (5)$$

By analogy to the theory of the wetting between three phases (solid, liquid and gas), θ is determined, in the case of heterogeneous crystallization, by the different interfacial tensions between the crystal nucleus, the substrate and the solution (two solids and a liquid), see Fig. 1, and depends on the affinity between the precipitating phase and the foreign substrate. As θ is varied between 0° and 180°, the better the contact, the lower the value of θ and ϕ.

2.3. Kinetics and mechanisms of growth

When nuclei have reached their critical size, the process of crystal growth succeeds the nucleation process.

Thermodynamically, the driving force of the crystallization process is the chemical potential change, $\Delta\mu$, expressed as a function of the supersaturation ratio Ω, see Equation 2. In the case of electrolytes and according to the solubility diagram (Fig. 2), deviation from the solubility isotherm is given by the expression: $IP^{1/\nu}K_{so}^{1/\nu}$, where IP is the ionic product, K_{so} the solubility product of DCPD at 37 °C, both expressed as a function of the activities, and ν the number of ions in the formula unit ($\nu = 2$ for $CaHPO_4.\ 2H_2O$). So, we defined the relative supersaturation ratio σ, for DCPD crystallization, as in Equation 6

$$\sigma = \Omega^{1/2} - 1 \quad (6)$$

Surface controlled electrolyte crystal growth mechanisms can be broadly divided into two categories: spiral growth and surface nucleation [10, 11]. Both may include volume diffusion as a limiting case. The overall growth rate is a combination of the bulk diffusion and the surface reaction processes. Mineralization reactions controlled by surface processes usually enable the growth rates to be expressed by the following simple empirical equation as a function of the relative supersaturation ratio σ [9]

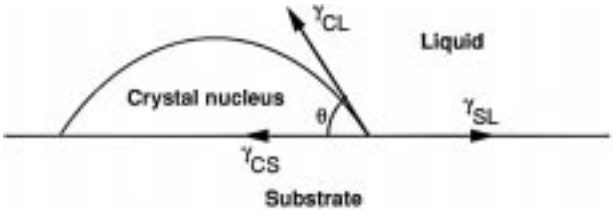

Figure 1 Representation of the wetting angle θ between the solution (liquid), the crystal nucleus and the foreign substrate and of the different interfacial tensions of this system.

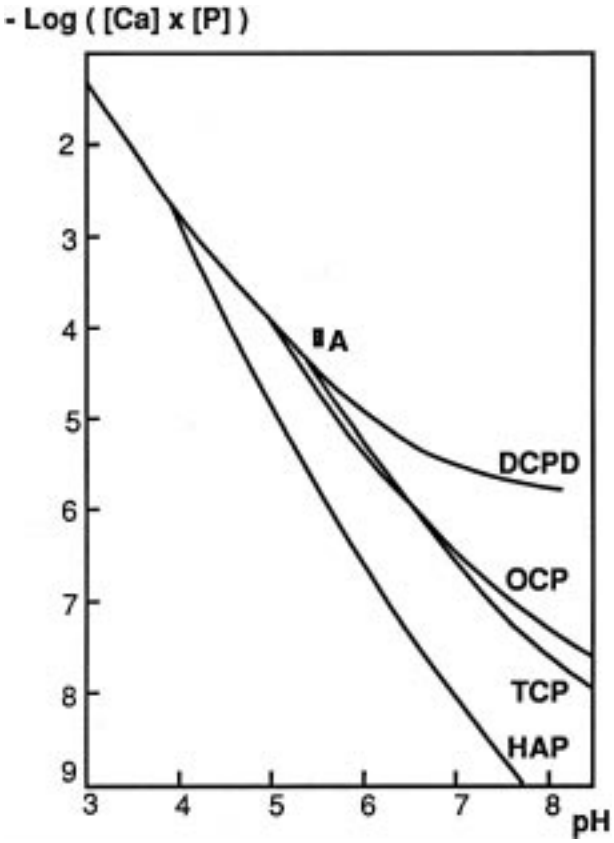

Figure 2 Calcium phosphate phase solubility isotherms as a function of pH at 37 ℃ and ionic strength = 0.1 mol l^{-1} DCPD = dicalcium phosphate dihydrate, OCP = octocalcium phosphate, TCP = tricalcium phosphate, HAP = hydroxyapatite.

$$Rc = ks\sigma^n \tag{7}$$

where k is the kinetic constant for a given temperature (Arrhenius type law), s is proportional to the number of active growth sites on the crystal surface and n the effective order of the reaction. The value of the kinetic order n indicates whether the mechanism is spiral growth ($n = 2$) or surface polynucleation ($n > 2$) [12, 13]. A value of $n = 1$ is usually attributed to bulk diffusion-controlled processes.

3. Materials and methods

3.1. The constant composition crystal growth technique

The constant composition crystal growth technique allowed the investigation of nucleation and growth processes with a sustained thermodynamic driving force. Using this method, developed by Tomson and Nancollas [14], we worked at exactly known supersaturations with a precision difficult to achieve by the conventional free drift technique. In Fig. 2, the calculated product log ([Ca] × [P]) of our work solutions is represented by the rectangular zone called A. The experimental set-up included a 250 ml double-walled glass reactor thermostated by circulating water, where the supersaturated solution was under low magnetic stirring, an impulsomat, a pH meter, two electrically coupled burettes and a recorder, see Fig. 3. The pH changes were detected by a combined glass electrode. The introduction of titanium particles in the supersaturated solution may initiate the formation of the first nuclei of calcium phosphate on the metal surface. When nuclei reached the critical size, they grew consuming ions of the supersaturated solution. The crystallization of calcium phosphate is accompanied by proton release in the solution. The small decrease in pH (ΔpH = $\pm$ 0.005), induced by the precipitation, controlled the simultaneous addition of the two titrant solutions with concentrations such that their addition exactly compensated for the phosphate and calcium ions precipitated and maintained the concentrations, pH and ionic strength constant. The titrant solutions contained, in one burette $CaCl_2 \cdot 2H_2O$ and KCl, and in the other burette KH_2PO_4 and KOH. The titrant burettes were connected to a recorder plotting the volume of titrant added against time.

3.2. Experimental conditions

All the experiments reported herein were performed at pH 5.50, $T = 37 \pm 0.1$ ℃, ionic strength = 0.1 mol l^{-1}, [Ca] = [P] = 8×10^{-3} to 9.5×10^{-3} mol l^{-1}, 10 mg of titanium powder (Aldrich 99.9%) were added to 100 ml of supersaturated solution.

The titanium powder particle size ranges were: < 20 μm, 20–45 μm, 63–90 μm and 90–125 μm. The BET (Brunauer–Emmet–Teller) specific surface areas, determined with nitrogen/helium flow in the proportion 30/70 (Micromeritics Flow Sorb II 2300), were 0.40, 0.19, 0.12 and 0.10 m^2 g^{-1}, respectively.

3.3. Characterizations

The products obtained after crystal growth were analyzed by X-ray diffraction and infrared spectroscopy: they were, in all cases, only composed of titanium and DCPD.

The morphology of the growing DCPD crystals was observed by SEM (Jeol JSM 6400).

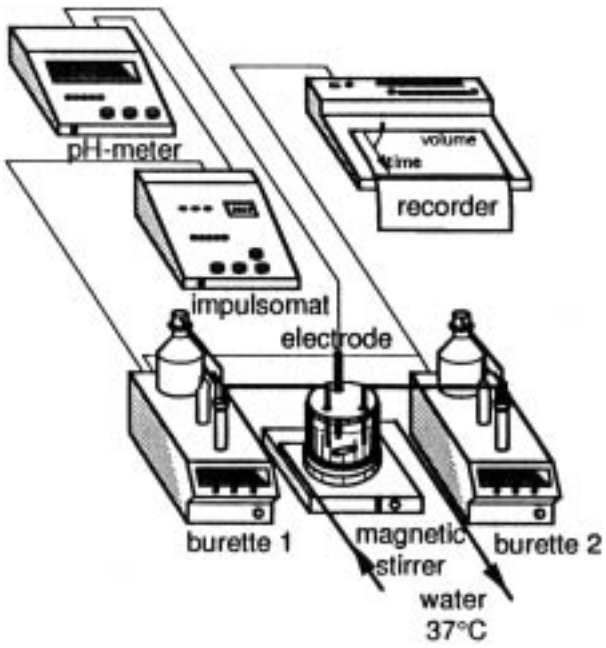

Figure 3 Constant composition crystal growth technique experimental set-up.

4. Results and discussion

4.1. Kinetic parameters

The induction time τ and the initial growth rate R_c were the two main parameters for the description of nucleation and growth processes respectively. τ corresponds to the time needed to form critical nuclei of calcium phosphate on the titanium powder surface or more precisely on the oxide layer on the surface of the metal [15]. The typical constant composition crystal growth experimental curve is shown in Fig. 4. Following an induction period, we can see a relatively rapid precipitation. The growth rate R_c ($\mathrm{mol\,min^{-1}\,m^{-2}}$) was calculated according to Equation 8

$$R_c = (\Delta V\, C)/(\Delta t\, m_0\, \mathrm{SSA}) \quad (8)$$

where ΔV/Δt is the curve tangent corresponding to a given percentage of the weight of DCPD precipitated compared to the initial titanium powder weight (generally for 0.3 ml added, corresponding to 25% growth, i.e. in a zone where the experimental curve is quite linear), C is the effective concentration of the titrant solutions with respect to the precipitating phase in $\mathrm{mol\,l^{-1}}$, m_0 the weight of titanium powder in g and SSA its specific surface area in $\mathrm{m^2\,g^{-1}}$. The growth rate R_c is in $\mathrm{mol\,min^{-1}\,m^{-2}}$. The induction time, τ (min), was determined at the intersection of the tangent with the x-axis. The experimental results of τ and R_c are reported in Table I. We have estimated the uncertainty on the determination of τ and R_c to 30 and 15%, respectively.

We can observe a third part on the experimental recording, for $V \geq 0.6$ ml, where the curve became exponential indicating a secondary nucleation phenomenon. This process induced an increase of the number of active growth sites in the crystallizing system leading to a strong enhancement of the reaction.

4.2. Estimation of the contact angle

According to Nielsen and Söhnel [16], the dependence of the induction time on the supersaturation ratio may be used to estimate the interfacial energy. We reported the estimation of the interfacial tension of DCPD grown on titanium, $\gamma_{het.}$, from the induction time experimental data, in a previous paper [17]. The average value calculated was $10.6\,\mathrm{mJ\,m^{-2}}$. Considering the expression of the free energy of critical nucleus formation, ΔG_c, in Equations 3 and 4, we can write the relation between the interfacial tension of homogeneous, $\gamma_{hom.}$, and of heterogeneous nucleation, $\gamma_{het.}$

$$\gamma_{het.}{}^3 = \phi\, \gamma_{hom.}{}^3 \quad (9)$$

$\gamma_{hom.}$ was calculated from the data given by Nielsen [10] in the case of the homogeneous nucleation of DCPD ($\gamma_{hom.} = 45\,\mathrm{mJ\,m^{-2}}$). Consequently, $\phi = 0.013$ and the contact angle was estimated at 30°. We can compare this contact angle to the one reported by Barone and Nancollas [18] for the study of the crystallization of DCPD on hydroxyapatite seeds: $\theta = 19.8°$. These results allowed the quality of titanium as a nucleating agent of DCPD to be evaluated. It seems that DCPD nucleates more easily on a compound of the same nature than on a totally foreign substrate such as titanium. As the calculated θ was quite low, titanium remained, however, a good substrate for the nucleation of DCPD.

TABLE I Induction time τ (min) and growth rate R_c ($\mathrm{mol\,min^{-1}\,m^{-2}}$) as a function of the titanium particle size and of the relative supersaturation ratio

		Titanium particle sizes (μm)							
		<20		20–45		63–90		90–125	
[Ca] (mM)	σ	τ	$R_c\ 10^4$	τ	$R_c\ 10^4$	τ	$R_c\ 10^4$	τ	$R_c\ 10^4$
8	0.26	269	1.4	252	3.5	335	4.7	277	7.5
8.5	0.33	124	3.35	90	9.6	110	15.5	80	21.3
9	0.40	47	6.8	49	14.6	44	27.9	54	41.5
9.5	0.47	42	10	28	22.3	30	41.5	28	64.4

($V_{total} = 100$ ml, $T = 37$ °C, pH = 5.50, mTi = 10 mg, [Ca] = [P]).

4.3. Crystallization kinetics and mechanisms

The formation of DCPD on the surface of the added titanium grains involved a nucleation step and the subsequent growth of the stable nuclei formed during the induction period. We can assume that there is competition between the nucleation of the calcium phosphate and its crystal growth until the titanium surface is completely covered by a layer of DCPD.

The logarithmic plot of R_c as a function of σ, according to Equation 7, is shown in Fig. 5, for each titanium particle size. The slope of each straight line gave the global order of the reaction n. The average value was 3.4 ± 0.4. This value could be interpreted as being indicative of a polynucleation mechanism [12]. But, based on the different characterizations by XPS spectroscopy (not presented) and also by SEM, of samples of titanium, this growth mechanism is not satisfactory.

Indeed, during the nucleation process, XPS analyses pointed out the formation of a calcium phosphate compound on the titanium surface. Moreover, Fig. 6 gathers scanning electron micrographs of samples of titanium withdrawn at different stages during the heterogeneous crystallization of DCPD and reveals, even at the end of the nucleation process, the presence of some platelets, which is the characteristic morphology of DCPD crystals, see Fig. 6b. The not well-crystallized

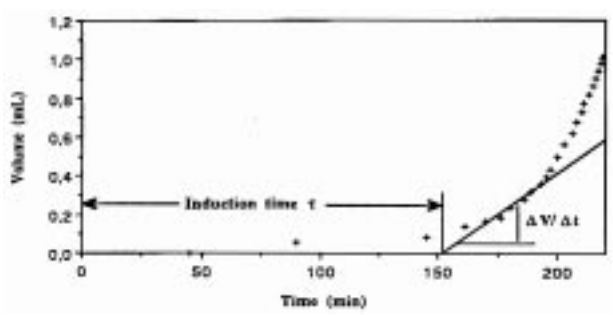

Figure 4 Experimental recording: plot of volume of titrants added as a function of time.

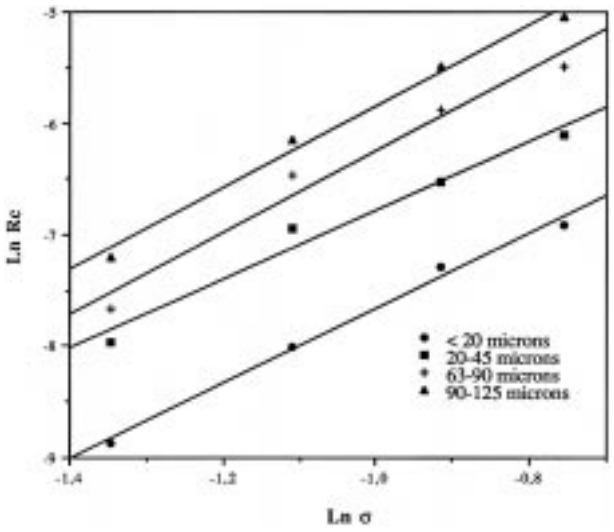

Figure 5 Plots of ln R_c versus ln σ for each titanium particle size.

calcium phosphate nuclei formed at the beginning of the nucleation stage (Fig. 6a), became more and more organized as time elapsed (Fig. 6b). Besides, the attachment of DCPD crystals to the titanium surface is clearly observed in Fig. 6c. Finally, as we can see on the last micrograph (Fig. 6d), of a sample withdrawn during the growth process, there are many crystals of brushite entirely covering the metal surface.

So, kinetically, we can assume that after the induction time, nucleation was completed and crystal growth of DCPD on DCPD became the preponderant phenomenon. Indeed, when the rate of growth was measured, there were already many DCPD platelets on the titanium surface and we were then reduced to the case of growth of DCPD on a layer of DCPD crystals located on the titanium surface.

A parabolic rate law has been encountered for the precipitation of many sparingly soluble salts [10]. Furthermore, in the literature, many authors studied the crystallization of DCPD and showed that the growth rate of DCPD on DCPD is described by the following simple growth rate equation: $R_c = K_s \sigma^2$, indicating a spiral growth mechanism [6, 19].

Considering the spiral growth model, we plotted $R_c^{1/2}$ versus σ, for each particle size (Fig. 7). We obtained a group of straight lines with a better correlation coefficient than in Fig. 5.

Furthermore, the graphical representation in Fig. 7 pointed out a minimal relative supersaturation ratio, σ_{min}, required to measure a growth rate different from zero. Indeed, whatever the size of the substrate, the abscissa at the intersection of the straight line with the x-axis, representing σ_{min}, was almost the same and equal to 0.14 ± 0.03. Experimentally, we noted that when σ was low ($\sigma < 0.19$), the induction period was very long ($\tau > 24$ h). With regards to the duration of our experiments, we can consider τ as infinite in this case.

If we assume that the driving force of the crystallization in the presence of foreign particles is not the supersaturation as expressed in Equation 7 but the excess of supersaturation $(\sigma - \sigma_{min})$ with regards to that needed to see crystal growth, we could consider a kinetic expression as in Equation 10.

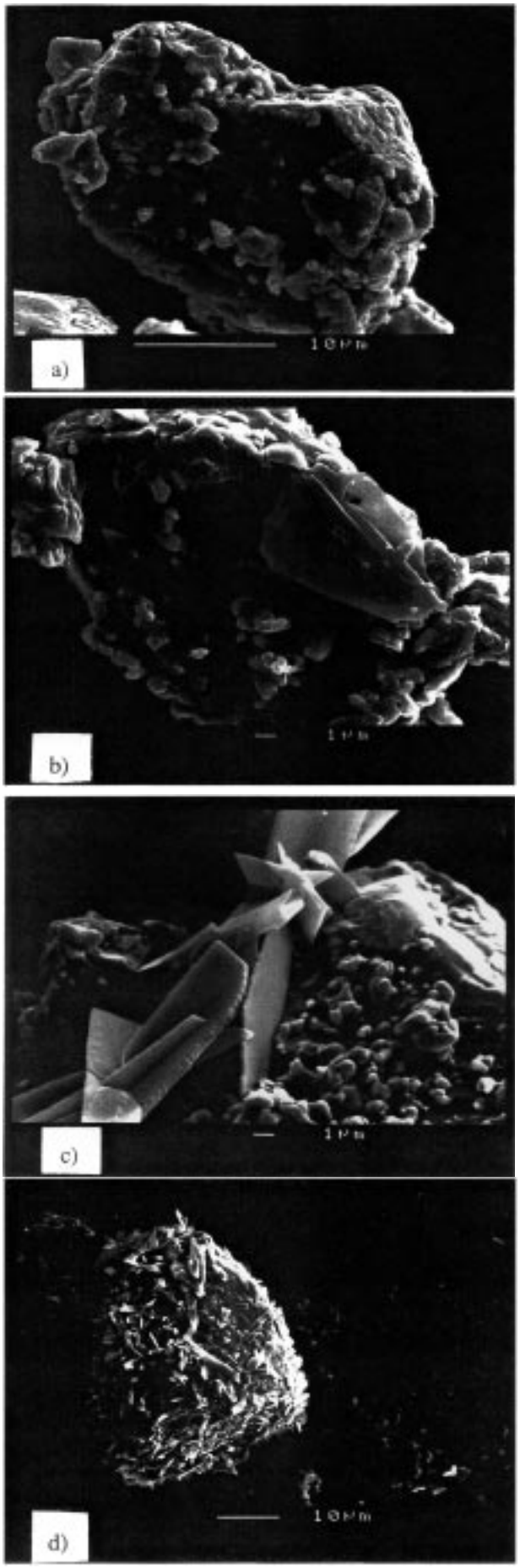

Figure 6 Scanning electron micrographs of samples of titanium withdrawn at different stages during the crystallization of DCPD. (a) at the beginning of the nucleation stage; (b) at the end of the nucleation stage; (c) at the beginning of the growth stage; (d) at the end of the experiment.

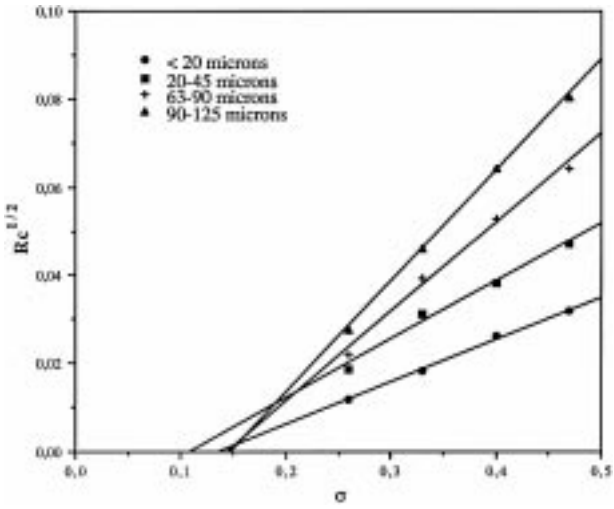

Figure 7 Plots of the initial growth rate squared versus the relative supersaturation ratio according to the spiral growth model.

$$R_c = K'_s(\sigma - \sigma_{min})^2 \quad (10)$$

with $\sigma_{min} = 0.14$ and where K'_s is the kinetic constant for a given temperature.

Even though their work concerned the growth of crystals on a seed of the same nature, we can refer to Francès *et al*. [20] who suggested a similar equation for the crystallization of sodium perborate in the presence of impurities. Besides, Boistelle and Astier [21] presented the theory of growth from solution in the presence of impurities inducing a shift of the crystallization curve, which remained parabolic as a function of supersaturation, toward larger supersaturations.

According to Equation 10, the determination of the slopes of the straight lines, in Fig. 7, allowed the calculation of K'_s. In Table II, the correlated expressions of kinetic laws are presented as a function of titanium grain size.

The two growth models discussed in this study accurately describe the experimental results, but with regards to the SEM observations, the XPS characterization and the correlation coefficient of the straight lines representing $R_c^{1/2}$ versus σ, Equation 10 seems to describe the growth process better. Furthermore, it is more realistic to consider that when a layer of DCPD crystals is formed on titanium, we must study the growth of DCPD on DCPD.

4.4. Effect of titanium particle size

For a given relative supersaturation ratio and considering the accuracy on the determination of the induction period (30%), it seemed that the nucleation process was independent of the substrate size, see Table I. In contrast, for a given range of titanium particle size, changes in relative supersaturation ratio strongly influence the induction time. We have reported the relation between the critical nucleus radius and the supersaturation ratio, see Equation 2. When the relative supersaturation ratio increased, r_c decreased enhancing the rate of nucleation; consequently the induction period decreased.

Figs 5 and 7 clearly show the size dependence of the growth rate of DCPD on titanium particle size and an increase of the growth rate with the size of the substrate.

TABLE II Kinetic laws as a function of titanium particle size for the spiral growth model

	$R_c = K$'s $(\sigma - \sigma_{min})^2$	
Particle sizes	R_c (mol min^{-1} m^{-2})	Correlation coefficient
< 20 μm	$9.2 \times 10^{-3} (\sigma - 0.14)^2$	0.998
20–45 μm	$1.74 \times 10^{-2} (\sigma - 0.11)^2$	0.994
63–90 μm	$4.08 \times 10^{-2} (\sigma - 0.15)^2$	0.995
90–125 μm	$6.35 \times 10^{-2} (\sigma - 0.15)^2$	0.999

The growth rate is expressed per area unit in order to cancel the effect of the specific surface area dispersion of the different titanium particle size ranges. Most theories of growth predicted a decrease of the growth rate with an increase of crystal size. This effect is related to a decrease of the SSA and of the number of growth sites, for a given weight of seed. Nevertheless, the opposite effect is observed in the present case and many authors also report the same type of variation for the homogeneous crystallization of various salts [22–24]. We could explain this phenomenon, at the scale of one particle, by the two-dimensional diffusion at the substrate surface that is facilitated when the particle offers a larger area. In the present work, it seems that the growth of DCPD is favored by large titanium particles and not by a large total area in solution. The surface reaction makes a large contribution to the growth process, with a surface diffusion dependence that increases with the size of the substrate. So, an increase of supersaturation and substrate size would probably enhance the growth rate.

Besides the observations mentioned in the previous paragraph, Fig. 7 reveals an increase of the slope, K'_s, with the size of the titanium particles. The value of K'_s seems to be strongly size-dependent (K'_s for particles of 90–125 μm was seven times higher than K'_s for particles of < 20 μm), see Fig. 8. As in the work of Jancic and Garside [24] concerning the growth of citric acid monohydrate crystals, the effect of titanium particle size on the kinetic constant has been correlated by a power law relation which fits the data rather well. For the range of titanium grain sizes used in this study, we found a parabolic law with a correlation coefficient of 1, see Equation 11

$$K'_s = 2.62 \times 10^{-6} L^2 + 2.49 \times 10^{-4} L + 6.51 \times 10^{-3} \quad (11)$$

with L the average size of titanium grain in μm.

If we combine the expression of the growth rate in Equation 10 and the effect of titanium particle size on the kinetic constant in Equation 11, we obtain the following rate equation with two parameters σ and L

$$R_c = (2.62 \times 10^{-6} L^2 + 2.49 \times 10^{-4} L + 6.51 \times 10^{-3}) \times (\sigma - 0.14)^2 \quad (12)$$

5. Conclusions

In the present work, the constant composition crystal growth method offers a rapid means of studying the

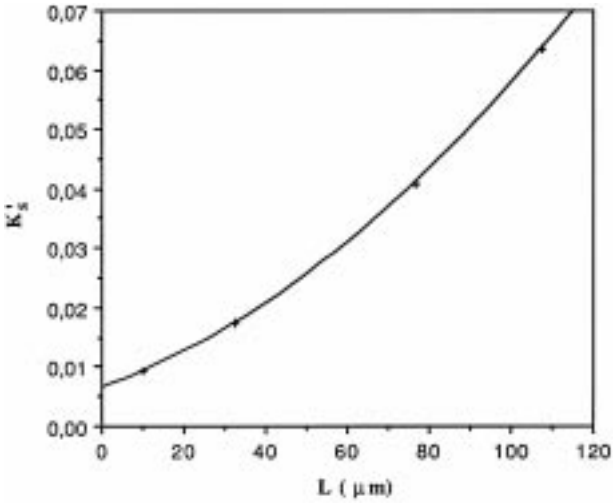

Figure 8 Correlation of the rate constant K's with the average size, L, of the titanium particles.

nucleation affinity of DCPD towards titanium surfaces. This method enabled precise measurements of induction time and growth rate for the heterogeneous nucleation and growth of DCPD on titanium particles of different sizes.

The nucleation data allowed us to determine the interfacial tension ($\gamma_{het.} = 10.6\,mJ\,m^{-2}$) and the contact angle between the crystal nucleus and the substrate ($\theta = 30^{\circ}$). The size of titanium grains does not influence the nucleation stage. On the other hand, the available data for DCPD growth rate indicate a marked dependence of the growth rate on substrate size.

From the kinetic results, it is clear that the mechanism involved is surface-controlled. Considering the limits of the technique in detecting the formation of the first crystals and especially the results of characterizations by XPS spectroscopy and SEM, we propose that it is more reliable to study the growth of DCPD on a layer of DCPD crystals, than on titanium. We showed that the spiral growth model rate equation is in good agreement with our experimental results when we introduce a minimum relative supersaturation ratio, σ_{min}, that takes into account the presence of foreign particles in the crystallizing system. Consequently, the proposed kinetic equation is expressed as a function of two parameters: the excess of supersaturation $(\sigma - \sigma_{min})$ which is squared and the size of the substrate L. It was shown that the correlation for the effect of titanium grain size, over the size range 0 to 125 μm, on the kinetic constant is described by a two-degree polynomial.

This work showed that titanium is a good substrate for the nucleation of calcium phosphate but we need to complete this series of experiments by using larger pieces of titanium metal resembling an actual prosthesis surface.

References

1. P. I. BRANEMARK, J. LINDSTRÖM, O. HALLEN, U. BREINE, P. H. JEPPSON and A. OHMAN, *Scand. J. Plast. Reconstr. Surg.* **9** (1975) 116.
2. B. KASEMO, *J. Prosthet. Dent.* **49** (1983) 832.
3. E. P. PASCHALIS, B. E. TUCKER, S. MUCKHOPADHYAY, K. WIKIEL, N. B. BEALS, J. A. BEARCROFT, M. SPECTOR and G. H. NANCOLLAS, in ''Hydroxyapatite and related materials'', edited by P. W. Brown and B. Constantz (CRC Press, London, 1994) p. 163.
4. M. D. FRANCIS and N. C. WEBB, *Calcif. Tissue Res.* **6** (1971) 335.
5. M. S. A. JOHNSSON and G. H. NANCOLLAS, *Crit. Rev. Oral Biol. Med.* **3** (1992) 61.
6. H. HOLH, P. G. KOUTSOUKOS and G. H. NANCOLLAS, *J. Crys. Growth* **57** (1982) 325.
7. J. C. HEUGHEBAERT, J. F. DE ROOIJ and G. H. NANCOLLAS, *ibid.* **77** (1986) 192.
8. P. G. KOUTSOUKOS and G. H. NANCOLLAS, *Colloids Surf.* **28** (1987) 95.
9. J. W. MULLIN, ''Crystallization'', 2nd ed. (Butterworths, London, 1972) p. 189.
10. A. E. NIELSEN, *J. Cryst. Growth* **67** (1984) 289.
11. W. B. HILLIG, *Acta Metall.* **14** (1966) 1868.
12. A. E. NIELSEN, ''Kinetics of precipitation''. (Pergamon Press, Oxford, 1964) p. 1.
13. G. H. NANCOLLAS and N. PURDIE, *Quart. Rev. Chem. Soc.* **18** (1964) 1–20.
14. M. B. TOMSON and G. H. NANCOLLAS, *Science* **200** (1978) 1059.
15. J. J. M. DAMEN, J. M. TEN CATE and J. E. ELLINGSEN, *J. Dent. Res.* **70** (1991) 1346.
16. A. E. NIELSEN and O. SÖHNEL, *J. Cryst. Growth* **11** (1971) 233.
17. C. COMBES, M. FRÈCHE and C. REY, *J. Mater. Sci.: Mater. Med* **6** (1995) 699.
18. J. P. BARONE and G. H. NANCOLLAS, *J. Colloid Interf. Sci.* **62** (1977) 421.
19. M. R. CHRISTOFFERSEN and J. CHRISTOFFERSEN, *J. Cryst. Growth* **87** (1988) 51.
20. C. FRANCÈS, B. BISCANS and C. LAGUÉRIE, *Chem. Eng. J.* **48** (1992) 119.
21. R. BOISTELLE and J. P. ASTIER, *J. Cryst. Growth* **90** (1988) 14.
22. A. G. JONES, J. BUDZ and J. W. MULLIN, *AIChE J.* **32** (1986) 2002.
23. E. T. WHITE, L. L. BENDIG and M. A. LARSON, *AIChE Symp. Series* **72** (1976) 41.
24. S. JANCIC and J. GARSIDE, in ''Industrial crystallization'', edited by J. W. Mullin (Plenum Press, New York, 1976) p. 363.
25. C. LAGUÉRIE and H. ANGELINO, in ''Industrial crystallization'', edited by J. W. Mullin (Plenum Press, New York, 1976) p. 135.

Received 12 August
and accepted 25 September 1997